

Gaia: a Window to Large Scale Motions

Adi Nusser¹

Physics Department and the Asher Space Science Institute-Technion, Haifa 32000, Israel

Enzo Branchini²

*Department of Physics, Università Roma Tre, Via della Vasca Navale 84, 00146, Rome, Italy
INFN Sezione di Roma 3, Via della Vasca Navale 84, 00146, Rome, Italy
INAF, Osservatorio Astronomico di Brera, Milano, Italy*

Marc Davis³

Departments of Astronomy & Physics, University of California, Berkeley, CA. 94720

ABSTRACT

Using redshifts as a proxy for galaxy distances, estimates of the 2D transverse peculiar velocities of distant galaxies could be obtained from future measurements of proper motions. We provide the mathematical framework for analyzing 2D transverse motions and show that they offer several advantages over traditional probes of large scale motions. They are completely independent of any intrinsic relations between galaxy properties, hence they are essentially free of selection biases. They are free from homogeneous and inhomogeneous Malmquist biases that typically plague distance indicator catalogs. They provide additional information to traditional probes which yield line-of-sight peculiar velocities only. Further, because of their 2D nature, fundamental questions regarding vorticity of large scale flows can be addressed. Gaia for example is expected to provide proper motions of at least bright galaxies with high central surface brightness, making proper motions a likely contender traditional probes based on current and future distance indicator measurements.

Subject headings: Cosmology: large scale structure of the Universe, dark matter

1. Introduction

In the standard cosmological paradigm, peculiar motions (i.e. deviations from Hubble flow) of galaxies are the result of the process of gravitational instability with overdense regions attracting material, and underdense regions repelling material. The coherence and amplitude of galaxy flows are a direct indication of the distribution of the dark matter, the cosmological background, and the underlying theory of gravity. Traditionally the

peculiar velocity field is derived from observations of distance indicators such as the Tully-Fisher relation (Tully & Fisher 1977) between luminosity and rotational velocity of galaxies. The observed flux and rotational velocity are then used to infer the distance from the TF relation. The distance is then subtracted from the redshift, cz , in order to obtain the line-of-sight component of the peculiar velocity of a galaxy, with a typical 1σ error $\sim 0.2 cz$.

Here we point out an alternative probe of the large scale velocity field by means of future likely measurements of proper motions of galaxies. As an example for such future measurements we con-

¹E-mail: adi@physics.technion.ac.il

²E-mail: branchin@fis.uniroma3.it

³E-mail: mdavis@berkeley.edu

sider the Gaia¹ space astrometric mission. Although the main aim of the mission is to study our Galaxy, Gaia will also be able to perform accurate astrometry for external galaxies, largely thanks to its excellent angular resolution, provided they are sufficiently distant (Perryman et al. 2001; Vaccari 2000). As an example, the nuclei of M87 at N5121, both at $d \simeq 17.8 h_{70}^{-1}$ Mpc, will be detected with apparent magnitudes $V \sim 16$ and $V \sim 14.7$, respectively, within an aperture of 0.65 arcsec , approximately corresponding to Gaia’s detection window (Ferrarese et al. 1994; Carollo et al. 1998; Lauer et al. 2007). With an expected end-of mission accuracy in the measurements of proper motions of $\sim (10 - 20) \mu\text{as yr}^{-1}$ at the V magnitudes of these two galaxies, Gaia will be able to measure the transverse displacements of these objects with an accuracy of $(0.8-1.6) 10^{-4} h_{70}^{-1} \text{ pc}$, corresponding to a transverse velocity $\sim 600 \text{ km s}^{-1}$, which is a rather typical value, comparable to that of the Local Group velocity with respect to the CMB. Although Gaia’s on board thresholding algorithm is optimized for stellar objects, a large number of galaxies will have their stellar light emission concentrated in a compact region (either a bulge or pseudo-bulge) of sub kpc in effective radius, sufficient to make them appear as detectable point-like sources (e.g. Kormendy 1977; Allen et al. 2006; Oohama et al. 2009; Graham 2011). Robin et al. (2012) estimates that Gaia will be able to detect $\sim 10^6$ galaxies. In fact, high surface brightness substructures within extended objects might be detected as individual sources associated to the same galaxy, hence improving the accuracy in the measurement of its peculiar motion, as we shall demonstrate in this paper.

Distances to galaxies are needed to derive their transverse peculiar velocities (in km s^{-1}) from the proper motions. High precision distances will become available for those star-forming galaxies that, once observed by Gaia, will subsequently have their Cepheid distances determined (for example by JWST²). However, these will be available for a limited number of relatively nearby galaxies, whereas we are interested in tracing the cosmic velocity field over large regions. As a proxy for the distance we will use the galaxy’s redshift,

which differs from the actual distance by the radial peculiar velocity. The relative error in the transverse velocity as a result of this approximation is small and decreases with redshift. An object with $V = 15$ will have an error in transverse velocity of $\sim 0.6 cz$. This is significantly larger than the uncertainty in line-of-sight peculiar velocities from distance indicators. However, we will show that the large number of galaxies expected to be observed with Gaia will beat the increased scatter, possibly making Gaia’s proper motions an excellent probe of the large scale flows. This probe of large scale flows is completely independent of any assumption on the intrinsic relations of galaxies. Further, the 2D transverse motions are orthogonal (in information content as well as in geometry) to standard line-of-sight peculiar velocities.

The outline of the paper is as follows. In §2 we present the general set up and describe theoretical tools for analyzing future transverse velocity data. We present, in §3, a rough estimate of the expected error in the transverse velocity obtained by smoothing individual velocities. Expected errors on astrometry for Gaia’s galaxies are discussed in §4 and a more general discussion on astrometry of extended objects is given in §5. In the concluding section §6, we present a general assessment of the transverse velocity data in comparison to other probes of large scale motions. We also discuss possible sources for redshifts of the population of galaxies expected to be observed by Gaia.

Unless otherwise specified, magnitudes observed by Gaia will refer to an aperture photometry 0.65 arcsec . They are given in the G band (350-1000 nm). Transformation from the more familiar V and I_c bands are performed using constant colors $V - G = 0.27$ and $V - I_c = 1$ for all galaxies (Fukugita et al. 1995; Jordi et al. 2010). We also assume that Gaia will identify all sources with $G < 20$ within 0.65 arcsec with 100 % completeness. Finally, we use $H_0 = 70 \text{ km s}^{-1}\text{Mpc}^{-1}$ to set the distance scale and use $h_{70} = H_0/70$ to parametrize uncertainties.

2. Methodology

We will assume an all-sky catalog of redshifts and proper motions. We denote the physical peculiar velocity by \mathbf{v} and the real space comoving

¹<http://sci.esa.int/science-e/www/area/index.cfm?fareaid=26>

²<http://www.jwst.nasa.gov/>

coordinate by \mathbf{r} , both expressed in km s^{-1} . Further, $v_{\parallel} = \mathbf{v} \cdot \hat{\mathbf{r}}$ and $\mathbf{v}_{\perp} = \mathbf{v} - v_{\parallel} \hat{\mathbf{r}}$ are, respectively, the components of \mathbf{v} parallel and perpendicular to the line-of-sight, where $\hat{\mathbf{r}}$ is a unit vector in the line-of-sight direction. We restrict the analysis to $cz \lesssim 15,000 \text{ km s}^{-1}$ and neglect cosmological geometric effects, so that the redshift coordinate is $\mathbf{s} = \mathbf{r} + v_{\parallel} \hat{\mathbf{r}}$. Note $\hat{\mathbf{s}} = \hat{\mathbf{r}}$ and $cz = r + v_{\parallel} = \mathbf{s} \cdot \hat{\mathbf{r}} = s$. Proper motions transverse to the line-of-sight will be denoted by $\boldsymbol{\mu}$. The transverse 2D space velocity is of a galaxy at real space distance r is

$$\begin{aligned} \mathbf{v}_{\perp} &= r\boldsymbol{\mu} \\ &= 677.22 \frac{\boldsymbol{\mu}}{1 \mu\text{as yr}^{-1}} \frac{r}{10^4 \text{ km s}^{-1}} h_{70}, \end{aligned} \quad (1)$$

which corresponds a transverse peculiar velocity of 474 km s^{-1} for $1 \mu\text{as yr}^{-1}$ at $d = 100 \text{ Mpc}$.

However, the true distances, r , are unknown, and, therefore, we make the approximation

$$\mathbf{v}_{\perp} = s\boldsymbol{\mu}. \quad (2)$$

This introduces a relative error v_{\parallel}/s in the determination of \mathbf{v}_{\perp} where $\langle v_{\parallel}^2 \rangle^{1/2} \sim 200 - 300 \text{ km s}^{-1}$ (Davis et al. 2011). Hence the error is negligible as we go to $s \gtrsim 2,000 \text{ km s}^{-1}$. The error is also random since $\langle \mathbf{v}_{\perp} v_{\parallel} \rangle = 0$.

Therefore, the estimated velocity field will be given as a function of the redshift space coordinate. To linear order, velocity fields expressed in real and redshift spaces are equivalent. In the quasilinear regime, dynamical relations can be derived for the velocity field in redshift space (Nusser & Davis 1994), thanks to the interesting property that an irrotational (or potential) flow in real space remain irrotational also in redshift space (Chodorowski & Nusser 1999).

2.1. From 2D transverse velocities to 3D flows

Here we offer basic expressions for the derivation of the full peculiar velocity field $\mathbf{v}(\mathbf{s})$ from the smoothed 2D transverse velocity field, $\mathbf{v}_{\perp}(\mathbf{s})$. Assuming a potential flow $\mathbf{v}(\mathbf{s}) = -\nabla\Phi(\mathbf{s})$ and expanding the angular dependence of Φ in spherical harmonics, $\Phi(\mathbf{s}) = \sum_{lm} \Phi_{lm}(s) Y_{lm}(\hat{\mathbf{s}})$, gives (Arfken & Weber 2005)

$$v_{\parallel} = -\sum_{lm} \frac{d\Phi_{lm}}{ds} Y_{lm} \quad (3)$$

$$\mathbf{v}_{\perp} = -\sum_{lm} \frac{\Phi_{lm}}{s} \boldsymbol{\Psi}_{lm}, \quad (4)$$

where $\boldsymbol{\Psi}_{lm} = r\nabla Y_{lm}$ is the vector spherical harmonic. Thanks to the orthogonality conditions $\int d\Omega \boldsymbol{\Psi}_{lm} \cdot \boldsymbol{\Psi}_{l'm'} = l(l+1) \delta_{ll'}^K \delta_{mm'}^K$, the potential coefficients can be recovered by

$$\Phi_{lm}(s) = \frac{-1}{l(l+1)} \int d\Omega \mathbf{v}_{\perp}(\mathbf{s}) \cdot \boldsymbol{\Psi}_{lm}(\hat{\mathbf{s}}), \quad (5)$$

for $l > 0$. This means that $\Phi(\mathbf{s})$ can be recovered from the \mathbf{v}_{\perp} up-to a monopole term which corresponds to a purely radial flow with zero transverse motions. That is not a serious drawback since the monopole term can always be removed from the predictions of any model to be compared with the data.

2.2. Testing the potential flow ansatz

Initial conditions in the early Universe might have been somewhat chaotic, so that the original peculiar velocity field was uncorrelated with the mass distribution, or even contained vorticity (e.g. Christopherson et al. 2011). At late time, a cosmological velocity field should have a negligible rotational component, \mathbf{v}^{rot} on large scale, away from orbit mixing regions. The reason is that any circulation, $\Gamma = \oint \mathbf{v}^{\text{rot}} \cdot d\mathbf{s}$, is conserved by Kelvin's theorem. Hence, any rotational component will be decaying as $1/a$, where a is the scale factor. In contrast, the irrotational component of the peculiar velocity will have a growing $v \sim \sqrt{a}$. Therefore, on large scales, away from collapsed objects, the irrotational component is expected to be negligible. The absence of any significant large scale vorticity is, therefore, a strong prediction of the standard cosmological paradigm. To assess this prediction, the observed transverse motions can be used to constrain the amplitude of the irrotational component. This can be done by writing the transverse component of \mathbf{v}^{rot} as (Arfken & Weber 2005)

$$\mathbf{v}_{\perp}^{\text{rot}} = \sum_{lm} V_{lm}^{\text{rot}} \boldsymbol{\Phi}_{lm}, \quad (6)$$

where $\boldsymbol{\Phi}_{lm} = \mathbf{s} \times \nabla Y_{lm}$ belong to another class of vector spherical harmonics that satisfy the same orthogonality conditions as $\boldsymbol{\Psi}$. Hence, V_{lm}^{rot} is equal to the r.h.s of Eq. 5 but with $\boldsymbol{\Phi}_{lm}$ instead of $\boldsymbol{\Psi}_{lm}$. Further, $\int d\Omega \boldsymbol{\Phi}_{lm} \cdot \boldsymbol{\Psi}_{l'm'} = 0$, hence the recovery of the rotational mode is formally independent of the potential flow mode.

3. The expected errors

We provide estimates of the expected random errors in the smoothed transverse velocity field, $\mathbf{v}_\perp(\mathbf{s})$, as a function of distance from the observer.³

The expected 1σ error, $\sigma_\mu(m)$, in the measurement of an object's proper motion depends on its G magnitude and, to a lesser extent, on its color (de Bruijne 2012). Hereafter, we will use σ_μ as a function of G , according to the expression referenced in de Bruijne (2012). This $\sigma_\mu(m)$ is plotted in the left panel of Fig. 1. Other possible error sources are photometric jitter from SNe, AGN and, for the latter sources, the presence of jets with large proper motions. We assume that spectrophotometry available for all objects detected by Gaia will significantly reduce the impact of these error sources which, therefore, will be neglected in the error budget.

The *rms* accuracy in the galaxy proper motion at redshift s can be obtained by summing over all galaxy magnitudes

$$\langle \sigma_m^{-2}(s) \rangle = \int_{-\infty}^{m_{lim}} n(m, s) \sigma_\mu^{-2}(m) dm. \quad (7)$$

We assume that the surface brightness [SB] profile of distant galaxies is sufficiently peaked to guarantee that a large fraction of the galaxy luminosity is within Gaia's detection window. The validity of this hypothesis will be discussed in Section 4. In this case the number density of galaxies $n(m, s)$, is simply related to the galaxy luminosity function $N(M)$: $n(m, s) dm = N(M) dM$, where $M = m - 5 \log_{10}(s) - 15$ is the absolute magnitude. For Gaia's G band, we approximate $N(M)$ by the Schechter form of the V band luminosity function with parameters given by (Brown et al. 2001). Other choices for the Schechter parameters of the V band luminosity function (Marchesini et al. 2012) do not change the results significantly at the magnitude limits considered here. The results for the average error are shown in the right panel for three magnitude cuts. The flatness of the curves

³ In generating the smoothed $\mathbf{v}_\perp(\mathbf{s})$ care must be employed since the transverse directions of galaxies in different sight-lines within a filtering window do not point in the same direction. This difficulty could be overcome by tensor window smoothing à la POTENT (Dekel et al. 1990). However, we will not be concerned with these fine details at this stage.

for all magnitude, is a reflection of the fact that number of galaxies increases strongly with magnitude.

Given individual measurements $\mathbf{v}_{\perp i} = \mathbf{v}_\perp(\mathbf{s}_i)$, we write the smoothed velocity as

$$\mathbf{v}_\perp(\mathbf{s}) = \frac{\sum_i \mathbf{v}_{\perp i} \sigma_{\perp i}^{-2} W(\mathbf{s}, \mathbf{s}_i)}{\sum_i \sigma_{\perp i}^{-2} W(\mathbf{s}, \mathbf{s}_i)} \quad (8)$$

where the summation is over all galaxies, $\sigma_{\perp i} = s \sigma_{\mu i}$ and W is a smoothing window function.

The 1σ errors on $\mathbf{v}_\perp(\mathbf{s})$ is given by

$$\sigma_\perp^2(\mathbf{s}) = \frac{\sum_i \sigma_{\perp i}^{-2} W^2(\mathbf{s}, \mathbf{s}_i)}{[\sum_i \sigma_{\perp i}^{-2} W(\mathbf{s}, \mathbf{s}_i)]^2}. \quad (9)$$

The summation over galaxies can be transformed into a volume integration with the same argument but multiplied by the number density of galaxies. Doing so for a uniform distribution and assuming a Gaussian window, W , of width R_G , we get

$$\sigma_\perp^2(s) = \frac{s^2}{8\pi^{3/2} R_G^3} \frac{1}{\langle \sigma_m^{-2}(s) \rangle}, \quad (10)$$

We have assumed the distant observer limit so that $|\mathbf{s}_i - \mathbf{s}| \ll s$. For a Top-Hat window of the same width we get the same expression but with $4\pi/3$ as the numerical factor in the denominator. Substituting $\sigma_\mu(m)$ (see left panel Fig. 1) in Eq. 10, we compute the expected error, σ_\perp , in the smoothed \mathbf{v}_\perp , for a gaussian smoothing with $R_G = 1, 500 \text{ km s}^{-1}$. The top panel in Fig. 2 shows curves of σ_\perp as a function of distance for three magnitude cuts.

For comparison the figure also plots the error in the filtered line-of-sight peculiar velocities in the SFI++ catalog of TF measurements of $\sim 4,000$ galaxies (Masters et al. 2006). There is a significance decrease in σ_\perp as the magnitude is increased from $G = 14$ to 15, but the improvement is not as dramatic when fainter galaxies with $15 < G < 16$ are included. The reason is the rapid deterioration in σ_μ at $G = 16$ which is not compensated by the added number of fainter galaxies. At redshifts $s \gtrsim 6,000 \text{ km s}^{-1}$ and for $G < 15$, peculiar velocities from Gaia's proper motions are expected to fair much better than the SFI++ catalog (Masters et al. 2006). Another important quantity which can be computed from transverse velocities is the dipole motion (i.e. bulk

flow) of spherical shells of a given thickness. This motion is described by a constant term \mathbf{B} and gives rise to a transverse velocity field of the form $\mathbf{v}_{\perp B} = \mathbf{B} - \hat{\mathbf{r}}(\mathbf{B} \cdot \hat{\mathbf{r}})$. The dipole term \mathbf{B} can be found by least squares fitting of $\mathbf{v}_{\perp B}$ to the observed velocities $\mathbf{v}_{\perp i}$. The expected error in \mathbf{B} as a function of distance of the shell, is plotted in the bottom panel in Fig. 2. Predictions for 3 magnitude cuts are plotted for spherical shells of $3,000 \text{ km s}^{-1}$ in thickness. For comparison we also plot the WMAP7 Λ CDM model (Larson et al. 2010) predictions for the amplitude of the velocity dipole on spherical shells. It is encouraging that the predicted amplitude is larger than the expected error out to relatively large distances.

4. Astrometry with Gaia’s galaxies

Here we provide a rough argument demonstrating the possibility of high precision astrometry with Galaxies observed by Gaia. To do this we use Gaia condition for astrometric measurements ($G < 20$ within an aperture of $\sim 0.65 \text{ arcsec}$) to define an analogous threshold based on SB. The mean SB of a $G = 20$ object within Gaia detection window is $\mu_G \sim 20 \text{ mag arcsec}^{-2}$. Here we shall make a more conservative choice and assume that only sources with $\mu_G < 18.5 \text{ mag arcsec}^{-2}$ will be used for astrometric purposes. A survey of the literature shows that this condition is satisfied for the central region of a significant fraction of galaxies (e.g. Kormendy 1977; Allen et al. 2006; Oohama et al. 2009; Balcells et al. 2007; Smith et al. 2009; Graham 2011; Ferrarese et al. 1994; Carollo et al. 1998; Lauer et al. 2007). For example, this can be seen in figure 3 in Oohama et al. (2009) showing a scatter plot of the B band effective SB versus half light radius for various galaxy types⁴. More importantly, we have visually inspected the observed V -band SB profiles of 200 out of ~ 600 galaxies in the Carnegie-Irvine Galaxy Survey (CGS; Ho et al. 2011; Li et al. 2011). Most of these galaxies are nearby (median distance of $\sim 25 h_{70}^{-1} \text{ Mpc}$) and with mean B -band absolute *total* magnitude of -20.2 , close to M_* . We identified galaxies reaching central SB of 18.5 mag/arc^2 and tabulated the corresponding

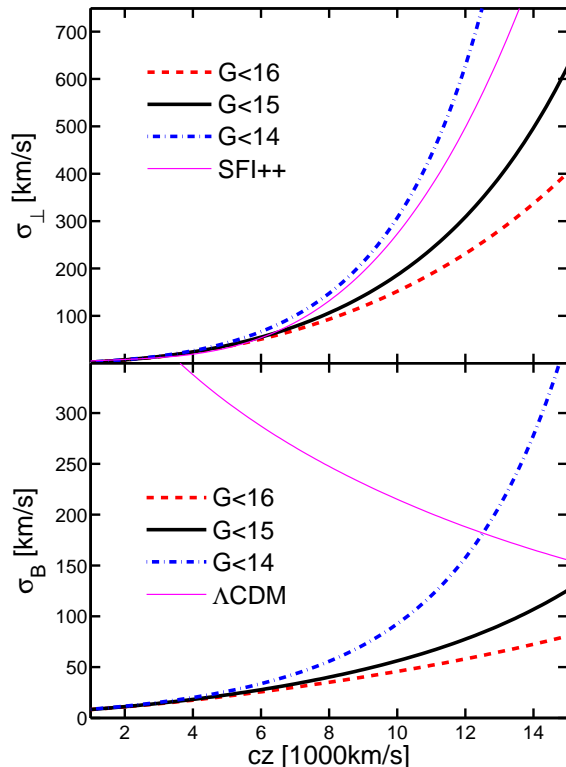


Fig. 2.— Expected errors (1σ) on two quantities computed from the Gaia astrometric galaxy data. *Top*: Errors in the 2D transverse peculiar velocity field obtained by filtering the data with a gaussian window of width $R_G = 1500 \text{ km s}^{-1}$. For comparison, the thin solid magenta line is the error in the SFI++ line-of-sight peculiar velocities smoothed with the same window. Errors scale like $R_G^{3/2}$. *Bottom*: Errors in the bulk (dipole) motion of spherical shells of thickness $\Delta cz = 3,000 \text{ km s}^{-1}$. Errors scale like $(\Delta cz)^{1/2}$. For reference, predictions from the WMAP7 Λ CDM for the dipole on shells are also plotted. In both panels, dash-dotted, solid and dotted curves correspond to $G=14, 15$ & 16 magnitude cuts, as indicated in the figure.

⁴For old stellar populations, $B \sim V + 1$ (Fukugita et al. 1995), and since $G = V + 0.27$, the astrometric condition $G \lesssim 18.5$ translates to $B \lesssim 19.7$.

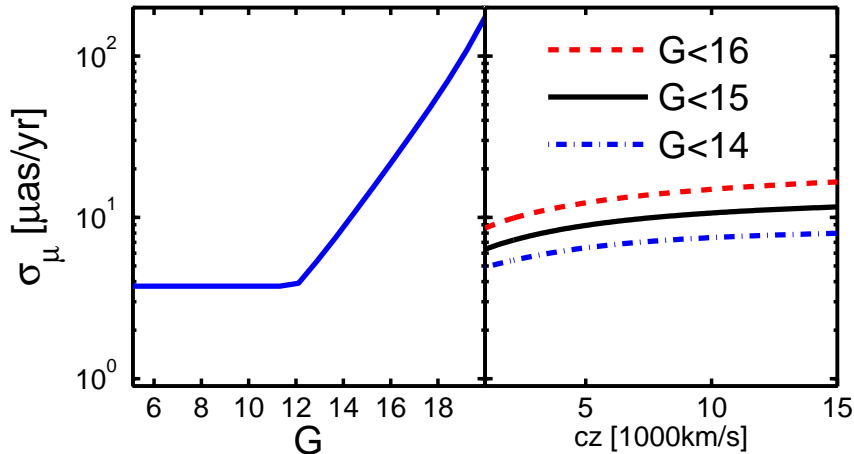


Fig. 1.— Expected error in Gaia’s proper motion measurements. *Left*: 1σ error of an object as a function of its G magnitude. *Right*: mean 1σ error of objects as a function of distant for three values of the G magnitude cut.

radii (in *arcsec*). Since we did not have access to the actual data the minimal radius we could determine using a ruler is $1 - 2$ *arcsec*. About 70% of the galaxies we inspected were brighter than $18.5\text{mag}/\text{arcsec}^2$ allowing them to be detected by Gaia. Since SB is a distance-independent quantity we can use this threshold to compute the maximum distance at which a galaxy would be detected in a single resolution element of Gaia. We find that the majority of early and late type galaxies could be detected as point sources at $G = 20$ if, respectively, placed at $\gtrsim 500 h_{70}^{-1}$ Mpc and $\gtrsim 250 h_{70}^{-1}$ Mpc. Overall, it looks like the overwhelming majority of early type galaxies and more than 50 % of late types will have peculiar motions measured by Gaia with errors in transverse velocities given in the top panel in Fig. 2. In addition, a significant fraction of their emitted light will be within Gaia’s detection window, which justify the simple relation between galaxy number density and luminosity function that we have adopted in Section 3. AGN will be easily detected by Gaia as bright, pointlike sources and possibly mistaken by galaxies. However, their contamination to a relatively local sample of objects with measure redshift, like the one we consider here, should be negligible.

In fact, since we are interested in studying the velocity field of the local ($\lesssim 100 h_{70}^{-1}$ Mpc) Uni-

verse the situation is likely to be even more favorable. Within this distance the typical galaxy will be resolved in high SB substructures that, if brighter than $G = 20$, can be detected as individual sources and analyzed as a group. Example of multiple high-SB sources are star forming regions, globular clusters and bulges with steep SB profiles that are more extended than Gaia’s window (for example, the SB-profile of M87 drops below $18.5\text{mag}/\text{arcsec}^2$ at $\sim 700 h_{70}^{-1}$ pc from the center. If placed at $\sim 50 h_{70}^{-1}$ Mpc it will be detected as ~ 10 individual sources by Gaia). Detecting multiple sources from the same objects significantly improves the astrometric precision, as we shall show in the next Section.

5. Astrometry with extended objects

The possibility of placing multiple constraints on the same objects allows, in principle, to improve the astrometric accuracy. We discuss this possibility in a general context and with a formalism that contemplate both the possibility of performing resolved photometry with high resolution instruments like HST⁵, JWST, LSST or Pan-STARRS (Saha & Monet 2005; Chambers 2005), and that of splitting an extended source in individual sources, like in the case of Gaia.

⁵<http://www.stsci.edu/hst/>

Suppose for simplicity we observe a galaxy at two different epochs, t_1 and t_2 . Let us define $I_i(\boldsymbol{\theta}_i)$ the SB of the object at the epoch t_i measured at the angular position of a pixel $\boldsymbol{\theta}_i$. In the case of traditional photometry $I_i(\boldsymbol{\theta}_i)$ represents the SB profile of the object at $\boldsymbol{\theta}_i$ whereas in the case of Gaia it represent the magnitude of the SB-substructure measured within the detection window. In principle the astrometric shift, \mathbf{p} , could be determined by minimizing, with respect to \mathbf{p} , $\chi^2 = \sum_i [I_1(\boldsymbol{\theta}_i) - I_2(\boldsymbol{\theta}'_i)]^2 / \sigma_i^2$ where the summation is over all pixels, $\boldsymbol{\theta}' = \boldsymbol{\theta} - \mathbf{p}$ and σ_{I_i} here is the 1σ error in the measurement of the SB (since \mathbf{p} is small we assume that σ_{I_i} in pixel i is the same for both images). We have assumed that I_1 and I_2 differ only by a linear displacement. In principle one should take into account changes in the internal structure of the object. Those, however, will have little effect compared to the overall observational accuracy. Since we will eventually be interested in the mean coherent displacement of an ensemble of many galaxies, incoherent changes in the internal structure of galaxies will be insignificant.

This procedure of minimizing the image differences exploits all information contained in both images but it requires a possibly non-trivial interpolation of $\boldsymbol{\theta}'$ on the observed pixel positions at $\boldsymbol{\theta}$. Therefore, we present here an alternative technique which alleviates this problem and clarifies additional matter related to the astrometric expected precision for extended objects. Suppose that the actual galaxy image at time t_1 , is described by $I_s(\boldsymbol{\theta}) = \sum_\alpha c_\alpha \tilde{I}^\alpha(\boldsymbol{\theta})$ where \tilde{I}^α are basis functions which may chosen to be orthonormal. Any choice (e.g. Fourier modes, wavelets) for \tilde{I} would do for our purposes here. The underlying image at t_2 is therefore $I_s(\boldsymbol{\theta} + \mathbf{p})$. The modeling in terms of the basis functions \tilde{I}^α should account that the signal is modulated by the PSF, while photometric noise is just white noise. The expansion coefficients c_α and the displacement \mathbf{p} are determined by minimizing

$$\begin{aligned} \chi^2 &= \sum_i \sigma_i^{-2} \left[I_{1i} - \sum_\alpha c_\alpha \tilde{I}_i^\alpha \right]^2 \\ &+ \sum_i \sigma_{I_i}^{-2} \left[I_{2i} - \sum_\alpha c_\alpha \left(\tilde{I}_i^\alpha + \frac{\partial \tilde{I}_i^\alpha}{\partial \boldsymbol{\theta}} \mathbf{p} \right) \right]^2. \end{aligned} \quad (11)$$

More generally, images are taken at many different epochs (about 70 epochs in the case of Gaia). Therefore, it is more appropriate to write $\mathbf{p} = \tilde{\boldsymbol{\mu}} t_k$ and to minimize the total χ^2 with respect to $\tilde{\boldsymbol{\mu}}$. Since the generalization is straightforward, for brevity of notation we adhere to the simple situation described by Eq. 11. We note that several variations of this procedure could be adopted. For example, as an alternative to minimizing χ^2 in Eq. 11, we could use basis functions defined in terms of $\boldsymbol{\theta} - \boldsymbol{\theta}_c$ where $\boldsymbol{\theta}_c$ is an assumed position comoving with a given point on the galaxy (e.g. the centroid in the case of a spherical object). We then could minimize the counterpart of the first term in Eq. 11 with respect to c_α and $\boldsymbol{\theta}_c$ to get $\boldsymbol{\theta}_c$ at epochs t_1 and t_2 . Using the same model for the images at the two epochs, the difference between $\boldsymbol{\theta}_c$ would then be the displacement \mathbf{p} . This will yield identical results to minimization of Eq. 11 of our choice of \tilde{I}^α given as functions of $\boldsymbol{\theta}$ rather $\boldsymbol{\theta} - \boldsymbol{\theta}_c$. The covariance matrix of the error in the estimated parameters c_α and \mathbf{p} is given by the inverse of the hessian of χ^2 formed from $H_{cc} = \partial^2 \chi^2 / \partial c_\alpha \partial c_\beta$, $H_{cp} = \partial^2 \chi^2 / \partial c_\alpha \partial \mathbf{p}$, and $H_{pp} = \partial^2 \chi^2 / \partial \mathbf{p} \partial \mathbf{p}$. It is easy to show that $|H_{cp}| \ll |H_{pp}|$, implying that the error on \mathbf{p} is H_{pp}^{-1} , i.e. almost independent of how well c_α are recovered. Considering a one dimensional displacement we get an error of $\sigma_p^2 \propto 1 / (\sum_i (dI_s/d\theta)^2 / \sigma_i^2)$. Assuming the objects' SB dominates the sky background so that $\sigma_{I_i}^2 \propto I_s$, we get

$$\sigma_p^2 \propto \frac{1}{f < (dI_s/d\theta)^2 / I_s^2 >}, \quad (12)$$

where f is the observed total flux of the object. Note that the averaged quantity $< (dI_s/d\theta)^2 / I_s^2 >$ is independent of the amplitude of I_s . Hence σ_p depends on the total observed flux and variance in logarithmic derivative of the SB. The actual value of the SB is irrelevant as long as it satisfies the detection criteria. The larger the fluctuations/irregularities in the stellar light, the more accurate is the astrometry. These irregularities may arise from different physical conditions in galaxies, e.g. spiral arms, young stellar associations, gravitational clumping of stars, caustics resulting from recent merging, and patchy intrinsic dust obscuration. In the case of Gaia, they will be seen as individual sources with a S/N ratio $\gtrsim 5$ at 1 arcsec^2 at SB of 20 mag arcsec^{-2} (Vaccari 2000).

For galaxies at $\lesssim 100 h_{70}^{-1}$ Mpc, SB fluctuations due to Poisson fluctuations in the finite number of (mainly hot luminous) stars per pixel (Blakeslee et al. 1999; Biscardi et al. 2008) may contribute as additional source of irregularities. It is interesting that a sufficiently patchy extended object brighter than $G \approx 12$ may yield more accurate astrometry of a point source with the same luminosity. The reason is the noise floor for point sources with $G \lesssim 12$. An extended object of the same luminosity but made of numerous patches each with $G > 12$ could therefore yield higher precision than the point source. We conclude that astrometry of extended objects could well be comparable to those of point sources.

6. Discussion

The number of galaxies expected to be observed by Gaia is likely to exceed standard distance indicator data by two orders of magnitude (Masters et al. 2006; Springob et al. 2012; Masters et al. 2008; Courtois et al. 2011). Pan-STARRS and LSST (Chambers 2005; Saha & Monet 2005) will yield a factor of 100 less accurate proper motions ($\sim mas yr^{-1}$) than Gaia, but they will have substantially more galaxies and therefore will also be useful for large scale motions. Despite the larger object-by-object error, the large number of galaxies in catalogs of proper motions make them a serious contender to traditional probes of the peculiar velocity field. The method has several advantages. Firstly, it is completely independent of any assumed intrinsic relations of galaxies and, hence, it does not suffer from the usual concerns related to these relations, e.g. linearity, selection biases and dependence on environment. Secondly, it yields the 2D transverse velocity component and hence it offers completely orthogonal information to standard probes which yield the line-sight-component. Thirdly, it is free from homogeneous and inhomogeneous Malmquist biases (Lynden-Bell et al. 1988).

The usefulness of the method for probing the 3D velocity field on scales of a few 10s of Mpc is limited to $s \lesssim 10,000 km s^{-1}$. However, large scale moments of the velocity field can be assessed at much larger distances. In particular the error of the dipole on (i.e. bulk flow of) spherical shells can be estimated with $\sim 100 - 200 km s^{-1}$ error

at $s \sim 15,000 km s^{-1}$. At larger redshifts, neither this method nor traditional ones are comparable to the constraints on the dipole from galaxy luminosities in future galaxy redshift surveys (Nusser et al. 2011). At lower distances ($< 2,000 km s^{-1}$) the transverse motions of galaxies could play an important role at providing new constraints on the motion of Local Group of galaxies.

Gaia will provide spectroscopic information of unresolved galaxies (Tsalmantza et al. 2012), especially those with a high SB nucleus that will be preferentially detected. However, the inferred redshifts may not be sufficiently accurate or available for all unresolved galaxies with astrometric data (e.g. Robin et al. 2012). The Two Mass Redshift Survey (2MRS; Huchra et al. 2011) offers redshifts of $\sim 4 \times 10^4$ galaxies down to $K_s = 11.75$. This is the deepest all-sky redshift catalog currently available. It was originally planned to reach $K_s = 12.2$ mag and to include $\sim 10^5$ galaxies. This is similar to the expected number of galaxies detected by Gaia brighter than $V = 15.27$ (i.e. $G = 15$). Further, since $K_s \approx K$ (Carpenter 2001) and $V - K \sim 2.7$ for most galaxies (Aaronson 1978), we conclude that the $K_s = 12.2$ 2MRS has the same objects' number density as the Gaia galaxies observed to $G = 15$, and undoubtedly it is largely the same sample. This is particularly interesting as Gaia's astrometric accuracy deteriorate rapidly at fainter objects. However, it is unclear if 2MRS will be continued to $K_s = 12.2$ in the very near future (Macri, private communication). For the purpose of the analysis presented here one could use a catalog of photometric redshifts based on the 2MASS galaxy catalog (Skrutskie et al. 2006), containing almost 1 million sources with $K_s < 13.5$ mag. Its current form (2MASS XSCz, Jarrett (2004)) offers distance errors as large as 20-25%, which will improve in the coming years using the data from other galaxy catalogs for the photo-z estimation (Bilicki, private communication).

We have restricted the error analysis here to $G \sim 15$ since redshifts will probably not be available for all fainter galaxies. However, data at fainter magnitudes can well be exploited by computing the dipole as a function of an effective depth corresponding to a certain magnitude range. This can then be compared with model predictions for an equivalent quantity (Bilicki et al. 2011).

7. Acknowledgments

We thank Maciej Bilicki and Gary Mamon for useful comments. This work was supported by THE ISRAEL SCIENCE FOUNDATION (grant No.203/09), the German-Israeli Foundation for Research and Development and the Asher Space Research Institute. MD acknowledges the support provided by the NSF grant AST-0807630. EB acknowledges the support provided by the Agenzia Spaziale Italiana (ASI, contract N.I/058/08/0) EB thanks the Technion Physics Department for the kind hospitality. AN is grateful for the hospitality of the Physics Department, Università Roma Tre. EB thanks Michele Bellazzini and Paola Parma for suggestions and discussions.

REFERENCES

- Aaronson, M. 1978, *ApJL*, 221, L103
- Allen, P. D., Driver, S. P., Graham, A. W., Cameron, E., Liske, J., & de Propriis, R. 2006, *MNRAS*, 371, 2
- Arfken, G. B., & Weber, H. J. 2005, *Mathematical methods for physicists* 6th ed. (Elsevier)
- Balcells, M., Graham, A. W., & Peletier, R. F. 2007, *ApJ*, 665, 1104
- Bilicki, M., Chodorowski, M., Jarrett, T., & Mamon, G. A. 2011, *ApJ*, 741, 31
- Biscardi, I., Raimondo, G., Cantiello, M., & Brocato, E. 2008, *ApJ*, 678, 168
- Blakeslee, J. P., Ajhar, E. A., & Tonry, J. L. 1999, *Post-Hipparcos Cosmic Candles*, 237, 181
- Brown, W. R., Geller, M. J., Fabricant, D. G., & Kurtz, M. J. 2001, *AJ*, 122, 714
- Carollo, C. M., Stiavelli, M., & Mack, J. 1998, *AJ*, 116, 68
- Carpenter, J. M. 2001, *AJ*, 121, 2851
- Chambers, K. C. 2005, in *Astronomical Society of the Pacific Conference Series*, Vol. 338, *Astrometry in the Age of the Next Generation of Large Telescopes*, ed. P. K. Seidelmann & A. K. B. Monet, 134
- Chodorowski, M. J., & Nusser, A. 1999, *MNRAS*, 309, L30
- Christopherson, A. J., Malik, K. A., & MatraVERS, D. R. 2011, *Physical Review D.*, 83, 123512
- Courtois, H. M., Tully, R. B., & Héraudeau, P. 2011, *MNRAS*, 415, 1935
- Davis, M., Nusser, A., Masters, K. L., Springob, C., Huchra, J. P., & Lemson, G. 2011, *MNRAS*, 413, 2906
- de Bruijne, J. H. J. 2012, *ArXiv1201.3238*
- Dekel, A., Bertschinger, E., & Faber, S. M. 1990, *ApJ*, 364, 349
- Ferrarese, L., van den Bosch, F. C., Ford, H. C., Jaffe, W., & O'Connell, R. W. 1994, *AJ*, 108, 1598
- Fukugita, M., Shimasaku, K., & Ichikawa, T. 1995, *PASP*, 107, 945
- Graham, A. W. 2011, *ArXiv:1108.0997*
- Ho, L. C., Li, Z.-Y., Barth, A. J., Seigar, M. S., & Peng, C. Y. 2011, *ApJ*, 197, 21
- Huchra, J. P., et al. 2011, *ArXi:1108.0669*
- Jarrett, T. 2004, *PASA*, 21, 396
- Jordi, C., et al. 2010, *A&A*, 523, A48
- Kormendy, J. 1977, *ApJ*, 218, 333
- Larson, D., et al. 2010, *ArXiv e-prints*
- Lauer, T. R., et al. 2007, *ApJ*, 664, 226
- Li, Z.-Y., Ho, L. C., Barth, A. J., & Peng, C. Y. 2011, *ApJ*, 197, 22
- Lynden-Bell, D., Faber, S. M., Burstein, D., Davies, R. L., Dressler, A., Terlevich, R. J., & Wegner, G. 1988, *ApJ*, 326, 19
- Marchesini, D., Stefanon, M., Brammer, G. B., & Whitaker, K. E. 2012, *ArXiv e-prints*
- Masters, K. L., Springob, C. M., Haynes, M. P., & Giovanelli, R. 2006, *ApJ*, 653, 861
- Masters, K. L., Springob, C. M., & Huchra, J. P. 2008, *AJ*, 135, 1738
- Nusser, A., Branchini, E., & Davis, M. 2011, *ApJ*, 735, 77

- Nusser, A., & Davis, M. 1994, *ApJL*, 421, L1
- Oohama, N., Okamura, S., Fukugita, M., Yasuda, N., & Nakamura, O. 2009, *ApJ*, 705, 245
- Perryman, M. A. C., et al. 2001, *A&A*, 369, 339
- Robin, A. C., et al. 2012, *ArXiv*1202.0132
- Saha, A., & Monet, D. 2005, in *Bulletin of the American Astronomical Society*, Vol. 37, American Astronomical Society Meeting Abstracts, 1203
- Smith, A. J., Loveday, J., & Cross, N. J. G. 2009, *MNRAS*, 397, 868
- Springob, C. M., et al. 2012, *MNRAS*, 2337
- Tsalmantza, P., et al. 2012, *A&A*, 537, A42
- Tully, R. B., & Fisher, J. R. 1977, *A&A*, 54, 661
- Vaccari, M. 2000, Master's thesis, Department of Astronomy - University of Padova - Italy / Osservatorio Astronomico di Padova - INAF